identical to the timewise input used for $H(\omega, t)$ in Eq. (7). Now, however, the relation between the longitudinal distance r traveled by the $0.7R$ station of the blade and the nondimensional time t must be derived. As seen from Fig. 1 the forward component of blade velocity at the $0.7R$ station is with the nondimensional time t (time unit $1/\Omega$)

$$dx/dt = V/\Omega + 0.7R \sin t \tag{12}$$

or integrated

$$x = Vt/\Omega - 0.7R \cos t + c \tag{13}$$

Setting $r = x_2 - x_1$ and assuming $t = 0$ for $x = x_1$ one obtains

$$r = Vt/\Omega - 0.7R \cos t \tag{14}$$

which inserted into Eq. (11) yields with $\omega\Omega = \omega_r V$ the timewise input

$$\lambda(t) = u(t) \exp i\omega[t - (0.7/\mu) \cos t] \tag{15}$$

If we interpret now $H(\omega, t)$ as the response to the delayed time input Eq. (15), the response covariance matrix is still given by Eq. (7). Numerically, using for example a Runge-Kutta integration routine for computing $H(\omega, t)$, the input Eq. (15) is as easily handled as the input without the time delay term $(0.7/\mu) \cos t$. However the filtered white noise method of Eqs. (9) and (10) is now not applicable. The problem can also be solved with the help of the nonstationary autocorrelation function. From Eq. (13) we have

$$r = x_2 - x_1 = (V/\Omega)(t_2 - t_1) - 0.7R(\cos t_2 - \cos t_1) \tag{16}$$

Inserting Eq. (16) into Eq. (1) one obtains

$$R_\lambda(t_1, t_2)/{\sigma_\lambda}^2 = \exp - |a(t_2 - t_1) - 1.4(R/L)(\cos t_2 - \cos t_1)| \tag{17}$$

The authors[6] have used a weighting function method to obtain the response covariance to the nonstationary random input process with the autocorrelation function Eq. (17). It was found that this method gave the same result as Eq. (7) with $H(\omega, t)$ from Eq. (15), however with a greater computational effort.

A numerical example used earlier[1] with rotor advance ratio $\mu = 1.6$, Lock number $\gamma = 4$, blade tip loss factor $B = 0.97$, blade flapping frequency ratio $P = 1.3$ was studied for a ratio of turbulence scale over rotor radius of $L/R = 4.0$, using Eq. (15) both with and without the time delay term $(0.7\mu)/\cos t$. It was found that the time variable flapping variance and the threshold crossing expectations for flapping in response to atmospheric turbulence were not substantially affected by the time delay term in Eq. (15). A typical turbulence scale at low altitude where turbulence is most severe is about $L = 400$ ft (Ref. 7). A value of $L/R = 4$ corresponds then to a rotor diameter of 100 ft which is much larger than for current or even for foreseeable future lifting rotors. It would then appear that the nonuniformity of the vertical turbulence velocity over the rotor disk is of little influence on the random blade flapping response, at least as far as longitudinal nonuniformity is concerned. This may not be true for more accurate blade representations including for example additional torsional and bending degrees of freedom, for which the preceding analysis remains valid. Also, lateral nonuniformity of the vertical turbulence velocity, because it is more elaborate to evaluate, has not been considered as yet.

References

[1] Gaonkar, G. H. and Hohenemser, K. H., "Stochastic Properties of Turbulence Excited Rotor Blade Vibrations," *AIAA Journal*, Vol. 9, No. 3, March 1971, pp. 419–424.

[2] Roberts, J. B., "Structural Fatigue under Non-Stationary Random Loading," *Journal of Mechanical Engineering Science*, Vol. 8, 1966, pp. 392–405.

[3] Van Trees, H. L., *Detection, Estimation and Modulation Theory*, Pt. 1, Wiley, New York, 1968.

[4] Gaonkar, G. H., "Interpolation of Aerodynamic Damping of Lifting Rotors in Forward Flight from Measured Response Variance," *Journal of Sound and Vibrations*, Vol. 18, No. 3, 1971, pp. 381–389.

[5] Wan, F. Y. M. and Lakshmikantham, C., "Rotor Blade Response to Random Loads: A Direct Time Domain Approach," AIAA Paper 72-169, San Diego, Calif., 1972.

[6] Gaonkar, G. H. and Hohenemser, K. H., "Comparison of Two Stochastic Models for Threshold Crossing Studies of Rotor Blade Flapping Vibrations," AIAA Paper 71-389, Anaheim, Calif., 1971.

[7] Gault, J. D. and Gunter, D. E., "Atmospheric Turbulence Considerations for Future Aircraft Designed to Operate at Low Altitudes," *Journal of Aircraft*, Vol. 5, No. 6, Nov.–Dec. 1968, pp. 574–577.

Panel-Flutter Analysis of a Thermal Protection-Shield Concept for the Space Shuttle

HERBERT J. CUNNINGHAM*

NASA Langley Research Center, Hampton, Va.

Nomenclature

A_{ij}^* = dimensionless generalized-aerodynamic-force matrix elements
B = number of panel segments
g = coefficient of nonviscous structural damping
$h_j(x)$ = shape of displacement mode j, length
I_s = mass moment of inertia of panel segment about its mass centroid, mass (length)^2/unit width
$\tilde{k}$ = spring stiffness at supports, force/unit displacement per unit width
k_s = reduced frequency based on l_s, $\omega l_s/V$
l_s = length of panel segment
M = Mach number of freestream
M_{ij}^* = dimensionless generalized-mass matrix element
m_s = mass of panel segment per unit width
Q_j = the mode-j aerodynamic-force term in the virtual-work series, force/unit width
$\bar{q}_j$ = generalized coordinate of displacement mode j
q_j = complex amplitude of $\bar{q}_j$
r_s = radus of gyration of panel segment about its mass centroid, length
U = elastic potential energy of the panel springs, force length/unit width
V = kinetic energy of the panel, force length/unit width
V = velocity of freestream, length/time
w = downwash at pnel surface, positive with z, length/time
w_j = the mode-j term in the series for w
x = streamwise coordinate, length
x_j = x-coordinate of segment juncture j ($j = 0, 1, \ldots, B$), length
z = vertical coordinate and vertical displacement of panel
z_j = the mode-j term in the series for z
Δp = lifting pressure, positive with z, force/unit area
δW = virtual work of the panel, force length/unit width
λ = dynamic pressure parameter $\rho V^2/M\tilde{k}$
μ = ratio of mass of panel segment to mass of air contained to a height of l_s over the segment, $m_s/\rho {l_s}^2$
ρ = density of airstream, mass/length^3
τ = time
Ω = flexibility eigenvalue, $(\omega_0/\omega)^2 (1 + ig)$
ω = circular frequency, time^{-1}
ω_0 = reference frequency, that of a mass m_s on a spring $\tilde{k}$, $(\tilde{k}/m_s)^{1/2}$, time^{-1}

Introduction

THE thermal protection shield of the space shuttle, like other structural elements, should be as low in weight as possible. This requirement leads to a need to insure the flutter safety of a shield during both launch and re-entry. The present Note describes a preliminary analysis based on a linear force-displacement relationship and piston-theory aerodynamic forces.

Received January 17, 1972; revision received February 25, 1972.

Index categories: Launch Vehicle and Missile Structural Design; Nonsteady Aerodynamics; Aeroelasticity and Hydroelasticity.

* Aerospace Technologist, Aeroelasticity Branch, Loads Division. Member AIAA.

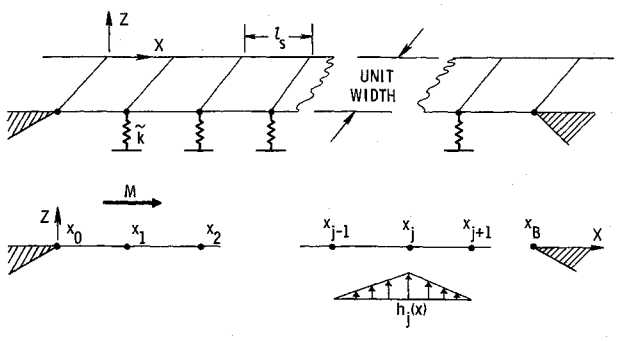

Fig. 1 Schematic diagram of panel analyzed.

The equations of dynamic equilibrium are developed on the basis of Lagrange's equations.

Analysis

The model analyzed is shown schematically in Fig. 1. It consists of a streamwise aligned array of uniform panel segments hinged together and supported above the load carrying structure on elastic supports that permit thermal expansion. Elastic deformations of the individual segments are negligible in comparison with the displacements at the elastic supports. The leading and trailing edges are simply supported. Cross-stream variations of motion and airflow are negligible compared to their streamwise variations. Thus, a streamwise strip of unit cross-stream width can be analyzed.

The degrees of freedom of the system are the displacements of the junctures of the segments. Thus the equilibrium equations for the various degrees of freedom will display mass coupling, but not elastic coupling.

The vertical displacement $z(x,\tau)$ is a series

$$z(x,\tau)=\sum_{j=1}^{B-1} z_j(x,\tau) \tag{1}$$

where

$$z_j(x,\tau)=\bar{q}_j(\tau)\,h_j(x)=q_j\,e^{i\omega\tau}\,h_j(x) \tag{2}$$

$$h_j(x)=\begin{cases} x-x_{j-1}; & x_{j-1}\leqq x\leqq x_j \\ -x+x_{j+1}; & x_j\leqq x\leqq x_{j+1} \\ 0\ ; & \text{otherwise}\end{cases} \tag{3}$$

The equilibrium equations are developed on the basis of Lagrange's equation

$$d/d\tau(\partial V/\partial\dot{z}_j)-\partial V/\partial z_j+\partial U/\partial z_j=Q_j;\quad j=1,2,\ldots,B-1 \tag{4}$$

The kinetic energy is given by

$$V=\tfrac{1}{2}m_s\sum_{j=1}^{B}[(\dot{z}_{j-1}+\dot{z}_j)/2]^2+\tfrac{1}{2}I_s\sum_{j=1}^{B}[(\dot{z}_j-\dot{z}_{j-1})/l_s]^2 \tag{5}$$

The potential energy consists entirely of the elastic potential energy of the spring supports, and is given by

$$U=\frac{\tilde{k}}{2}\sum_{j=1}^{B-1} z_j^{\,2} \tag{6}$$

The aerodynamic forces are those from piston theory

$$\Delta p/\rho V^2/2=(-2/M)w/V \tag{7}$$

where the downwash at the surface is

$$w=(V\,\partial/\partial x+\partial/\partial\tau)z \tag{8}$$

For simple harmonic motion, and with l_s used as a reference length

$$w/V=(\partial/\partial x+i\omega l_s/V)z/l_s=\sum_j w_j/V \tag{9}$$

where

$$w_j/V=q_j\,e^{i\omega\tau}\,[\partial h_j(x)/\partial x+(i\,\omega l_s/V)\,h_j(x)/l_s] \tag{10}$$

From Eq. (3)

$$\frac{\partial h_j(x)}{\partial x}=\begin{cases} 1; & x_{j-1}\leqq x<x_j \\ -1; & x_j<x\leqq x_{j+1} \\ 0; & \text{otherwise}\end{cases} \tag{11}$$

The virtual work δW done by the aerodynamic forces acting through the virtual displacements δq_j is

$$\delta W=\sum_j Q_j\,\delta q_j=\int_0^{x_B}\Delta p\sum_{j=1}^{B-1} h_j(x)\,\delta q_j\,dx \tag{12}$$

$$Q_j=e^{i\omega\tau}\frac{\rho V^2}{2}\left(\frac{-2}{M}\right)\frac{l_s^{\,2}}{6}\{q_{j-1}(-3+ik_s)+q_j(4ik_s)+q_{j+1}(3+ik_s)\} \tag{13}$$

Application of Eqs. (5, 6, and 13) into Eq. (4) leads to the equilibrium equations

$$-\omega_2^{\,2}\,e^{i\omega\tau}\frac{m_s}{2}\left[\frac{l_s}{3}q_{j-1}+\frac{4}{3}l_s q_j+\frac{l_s}{3}q_{j+1}\right]+e^{i\omega\tau}\tilde{k}l_s q_j+e^{i\omega\tau}\frac{\rho V^2}{2}\frac{2}{M}\frac{l_s^{\,2}}{6}[(-3+ik_s)q_{j-1}+4ik_s q_j+(3+ik_s)q_{j+1}]=0;$$

$$j=1,2,\ldots,B-1 \tag{14}$$

Dropping the time dependence term $e^{i\omega\tau}$, and dividing the equations by $(-\omega^2 l_s m_s)$ gives in matrix form

$$\left[[\,-\Omega\,]+[M_{ij}^*]-\frac{1/\mu}{6Mk_s^{\,2}}[A_{ij}^*]\right]\{q_j\}=\{0\} \tag{15}$$

where the dimensionless generalized mass elements are

$$M_{ij}^*=\begin{cases}\frac{2}{3}; & j=i \\ \frac{1}{6}; & j=i\pm1>0 \\ 0; & \text{otherwise}\end{cases} \tag{16}$$

the dimensionless generalized aerodynamic-force elements are

$$A_{ij}^*=\begin{cases}4ik_s & ;j=i \\ \pm3+ik_s; & j=i\pm1>0 \\ 0 & ;\text{otherwise}\end{cases} \tag{17}$$

(in which the subscript index i is not to be confused with the unit of imaginaries $i\equiv(-1)^{1/2}$ and the complex flexibility eigenvalue has the form

$$\Omega\equiv(\omega_0/\omega)^2(1+ig)$$
$$\omega_0^{\,2}\equiv\tilde{k}/m_s \tag{18}$$

where g is directly interpretable as the coefficient of structural damping (nonviscous internal friction) that is uniform for all springs. This form of Ω is chosen because it provides a means of accounting for structural damping as it is often used in flutter analysis. The same form of Ω would appear if either a complex stiffness had been carried through the analysis, or a nonpotential dissipation function had been used.

For a choice of M, k_s, and B the set of eigenvalues Ω and eigenvectors $\{q_i\}$ can be calculated by using an eigenvalue subroutine for complex non-Hermitian matrices.

A dynamic-pressure parameter is defined as

$$\lambda\equiv\frac{\rho V^2}{M\tilde{k}}=\frac{1}{M\,Re(\Omega)}\frac{1/\mu}{k_s^{\,2}} \tag{20}$$

and a set of λ corresponding to the set Ω is readily calculated.

Results

A representative result is shown in Fig. 2 for $M=2.0$, $k_s=0.6$, and $B=10$. Plotted against the mass ratio $1/\mu$ are the curves of λ and of the associated g values. As $1/\mu$ increases from 0 (for $\rho=0$) all nine roots depart initially into the negative g region indicating flutter stability. A further increase of $1/\mu$ causes an instability of three of the roots (in the range shown) as g becomes positive. In this case, the roots with the two lowest values of $1/\mu$ have closely equal values of λ that are the lowest and therefore critical. The real and imaginary parts of the complex mode shape

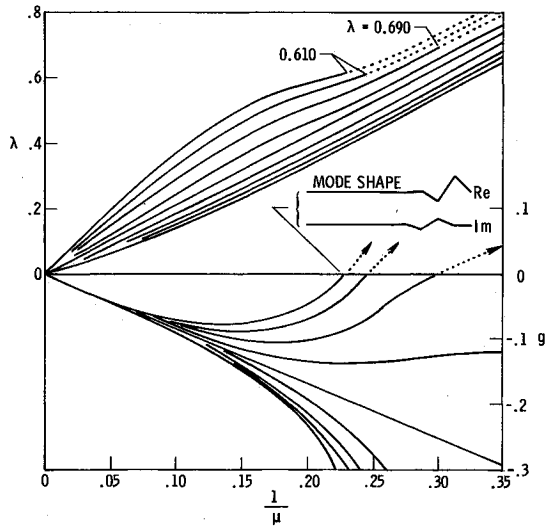

Fig. 2 Plots of dynamic pressure parameter λ and associated structural damping coefficient g vs mass ratio $1/\mu$, for $M = 2.0$, $B = 10$, and $k_s = 0.6$.

at an indicated point of neutral flutter stability are also shown. The segment juncture closest to the trailing edge has the largest amplitude, while the forward 60% has very small amplitude. This flutter mode shape is typical of the present analytical results.

The use of other Mach numbers verifies that combinations of $1/\mu$ and M that give the same ratio $1/\mu M$ give identical results. Figure 3 gives flutter boundaries plotted against $1/\mu M$ that are essentially coincident for $B = 4$, 10, and 20. These boundaries are, of course, the loci of the neutral stability points for $g = 0$ with the lowest λ for a range of $k_s = 0.0$ to about 1.0. The point from Fig. 2 is labeled. The flutter boundary slopes upward to the right because of the aerodynamic-damping term in the piston theory. The result of using only the static slope term in the downwash of Eq. (9) is shown by the horizontal boundary labeled "static aerodynamics only."

The small crosshatched region in the lower left of Fig. 3 covers the region of expected maximum dynamic pressure during launch, using the $\bar{k}$ and m_s of a candidate design being studied.

Conclusions

The panel flutter characteristics of a candidate thermal protection system (TPS) for the space shuttle have been analyzed based on piston theory aerodynamics and Lagrange's equations. The panel was analyzed as being simply supported at leading and trailing edges and made up of a number of uniform rigid segments hinged together and supported on springs at the segment junctures. For zero structural damping, a single flutter boundary of dynamic pressure parameter vs a mass ratio parameter was found to apply for all Mach numbers to which piston theory is applicable. A variation in the number of panel segments from 4 to 20 was found to have practically no effect on the flutter boundary. Use of the parameters of a conceptual design being studied for the TPS along with the maximum launch dynamic pressure and the associated Mach number predicts the TPS candidate panel array to be deep in the "no-flutter" region during launch and, therefore, safe from panel flutter.

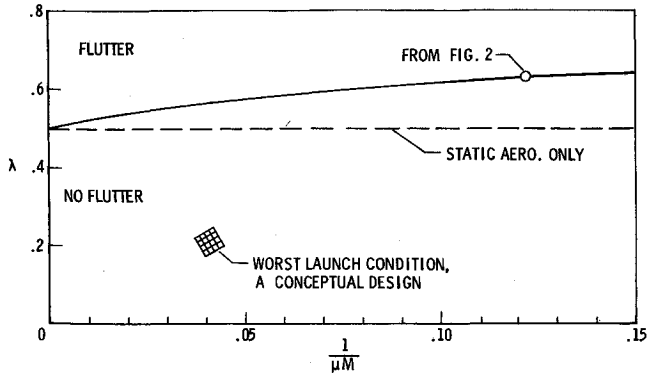

Fig. 3 Flutter boundary of λ vs $1/\mu M$ for $B = 4$, 10, and 20 with and without the aerodynamic damping of piston theory.

Application of Rice's Exceedance Statistics to Atmospheric Turbulence

WEN-YUAN CHEN*
NASA Langley Research Center, Hampton, Va.

Introduction

THE exceedance statistics of atmospheric turbulence have a direct bearing on the analysis of dynamic response of aircraft structures. The basic concepts of the theory of exceedance statistics are due to Rice.[1] He has derived a simple, yet important equation for the prediction of expected number of times per second, $N(\alpha)$, that the random disturbance will cross the value α. In order to apply his equation, the random fluctuation ought to be a stationary Gaussian process. In the literature, the velocities in individual patches of turbulence encountered by aircraft under different atmospheric conditions have been reported as stationary and Gaussian[2-4] to a sufficient extent to permit many practical applications. The estimation of exceedance statistics by Rice's equation was considered one of such.

Recent evidence,[5] however, indicates that there is disagreement between the measured exceedance values and the theoretical predictions given by Rice's equation. In an unpublished paper, R. Steiner, Langley Research Center, has suggested that the discrepancy may be due to the effect of multiple inputs to the airframe or due to the nonlinear response of the aircraft. In Ref. 5, it was suggested that nonstationary time trends in the data sample may cause the discrepancy. The purpose of the present work is to offer another explanation and to present some experimental evidence to support it.

Atmospheric turbulence is in general not a stationary nor a normal process. However, for a particular patch of turbulence or a segment of the patch, it might be fairly stationary both in the mean and in the variance. For such turbulence, the first-order distribution will usually appear to have a rather good Gaussian form. Yet, its second-order distribution will invariably turn out to be non-Gaussian, as will be evident later, indicating strongly that the turbulence is not a Gaussian process. It is emphasized that Rice's equation is built on the premise that the second-order distribution of a random process is joint-normal. It is then obvious that the application of Rice's exceedance statistics to atmospheric turbulence is bound to produce a discrepancy, regardless of the fact that the process is stationary and its first-order distribution is normal.

Theoretical Considerations

In order to stress the point that good Gaussian appearance of the first-order distribution alone is not adequate to insure a successful application of Rice's formula, let us study carefully the fundamental assumptions behind it. We shall adopt the route developed by Papoulis[6] to arrive at Rice's simple result in order to examine the assumptions involved. By adopting Papoulis'

Presented as Paper 72-136 at the AIAA 10th Aerospace Sciences Meeting, San Diego, Calif., January 17–19, 1972; submitted January 3, 1972; revision received March 28, 1972.

Index category: Aircraft Gust Loading and Wind Shear.

* NRC-NASA Resident Research Associate.